Vol. 6, No. 1, Spring 2021, pp. 53-69
دوره ششم، شماره ۱، بهار ۱۴۰۰، صفحه ۵۳ تا ۶۹

نشریه مهندسی منابع معدنی
Journal of Mineral Resources Engineering (JMRE)

DOI:10.30479/jmre.2021.14434.1459

Research Paper

The Effect of Temperature and Heating–Cooling Cycles on Mode I, Mode II and Mixed-Mode I-II Fracture Toughness of Sandstone

Latifi Sh.[1], Hosseini M.[2*], Mahdikhani M.[3]

1- M.Sc Student, Dept. of Mining Engineering, Imam Khomeini International University, Qazvin, Iran
2- Associate Professor, Dept. of Mining Engineering, Imam Khomeini International University, Qazvin, Iran
3- Assistant Professor, Dept. of Civil Engineering, Imam Khomeini International University, Qazvin, Iran

(Received: 26 Oct. 2020, Accepted: 23 Jan. 2021)

Abstract

In the case of explosions and fires, the rocks undergo a cycle of heating and cooling. For that, first, they are exposed to considerable heat and then cooled after extinguishing the fire. Temperature variations and subsequent contraction and expansion affect the physical and mechanical properties of rocks. Through two series of tests, the effects of temperature and the number of heating-cooling cycles on the mode I, mode II and the effective mixed-mode I-II fracture toughness of Lushan sandstone were investigated. In the first series, the effect of temperature was studied in a heating–cooling cycle at ambient temperature (25°C) and 60, 150, 200, 300, 500, and 700°C. The highest and lowest mode I, mode II and the effective mixed-mode I-II fracture toughness were, observed at 150 and 700°C, respectively. In the second series of tests, the effect of the number of heating–cooling cycles was investigated on the mode I, mode II and the effective mixed-mode I-II fracture toughness of sandstone specimens at 150°C (for hydraulic fracturing modeling) and a crack inclination angle of 45°. According to the results, the mode I, mode II and the effective mixed-mode I-II fracture toughness increased in the first cycle and decreased with increasing the number of heating–cooling cycles. As the crack inclination increased, the effective mixed-mode I-II fracture toughness of the sandstone specimens increased. The mode II fracture toughness increased up to a crack inclination angle of 45° and then decreased. Moreover, the mode of fracture changes from opening mode (mode I) at the crack inclination angle of zero degree to mixed mode (tension-shear) at the crack inclination angle of less than 28.8°. The mode of fracture changes from tensile-shear to compression-shear at the crack inclination angle of greater than 28.8°.

Keywords

Fracture toughness, Heating–cooling cycle, Mixed-mode, Sandstone, Crack inclination angle.

Corresponding Author, Email: ma.hosseini@eng.ikiu.ac.ir

1- INTRODUCTION

Fracture mechanics is one of the branches of mechanics engineering concerned with the study of the propagation of cracks in rocks. From a microscopic point of view, crack growth occurs due to the separation of molecular bonds at the crack tip. Fractures of rock are created by the presence of a large number of pores and cracks. When an external force is applied to the rock, microcracks are formed and propagated, leading to macro-fractures and eventually rock fracture [1].

In recent years, significant progress has been made in fracture mechanics, which can be attributed to the wide range of engineering problems (such as drilling bits and tunnel-boring machines disc cutters) that strengthen this scientific field undoubtedly [2,3]. According to the fracture mechanics definition, unstable fracture occurs when tension is concentrated near the crack tip. In this case, one of the stress intensity factors, namely the mode I factor (K_I), the mode II factor (K_{II}) or the mixed-mode factor, reaches a critical value of K_{IC} or K_{IIC}. This critical value, called fracture toughness, in fact shows the ability of rocks to withstand crack formation and propagation. Depending on the type of loading, three crack propagation modes including the mode I, mode II and mode III may be observed during fracturing based on the geometry and loading. Any combination of these three basic modes can be considered a mixed-mode [4]. It is observed that as cracks travel faster in brittle solids such as glass, rocks and rock-like materials, they tend to branch out [5].

Various methods are available for determining the fracture toughness of rock specimens. The conventional test on the cracked straight through Brazilian disc (CSTBD) specimens was used to determine the mixed-mode I-II fracture toughness. This method was independently used by Awaji and Sato [6] and by Sanchez based on previous studies by Bariman and Sanchez [7]. This test was then used and supported by Atkinson *et al.* [8] and Chong and Kuruppu [9] for determining the fracture toughness using the straight notched Brazilian disc (SNBD) specimens. Due to the widespread application of the Brazilian disc in determining fracture mechanisms including the mode I, mode II and mixed-mode I-II fracture, the SNBD specimens were used in this study to determine the mixed-mode I-II fracture toughness of sandstone (Figure 1).

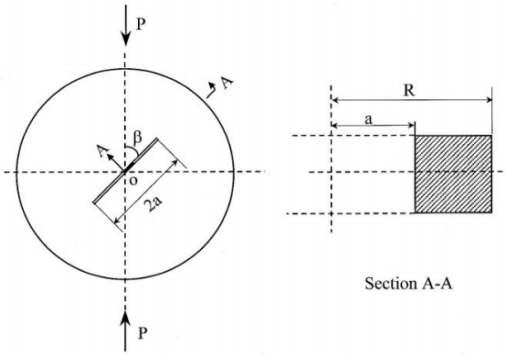

Figure 1. The schematic representation of the SNBD geometry [10]

Equations 1 and 2 proposed by Atkinson *et al.* [6] and Equation 3 suggested by Funatsu *et al.* [11] were used to calculate the stress intensity factors and the mode I, mode II, and mixed-mode I-II fracture toughness.

$$K_{Ic} = \frac{P\sqrt{a}}{\sqrt{\pi}RB} N_I \quad (1)$$

$$K_{IIc} = \frac{P\sqrt{a}}{\sqrt{\pi}RB} N_{II} \quad (2)$$

$$K_{eff} = \sqrt{K_{Ic}^2 + K_{IIc}^2} \quad (3)$$

Where:

K_{IC}, K_{IIC} and K_{eff}: represent the mode I, mode II and the effective mixed-mode I-II fracture toughness respectively,

R: the Brazilian disc radius,

B: disc thickness,

P: pressure load at fracture point,

a: half-length of the crack,

N_I and N_{II}: denote the dimensionless intensity factors which are dependent on a/R and β (loading angle relative to the crack direction).

Equations 4 and 5 were proposed by Atkinson *et al.* [6] to determine N_I and N_{II} for a/R<0.3:

$$N_I = 1\text{-}4\ (\sin\beta)^2 + 4\ (\sin\beta)^2 * (1\text{-}\ 4(\cos\beta)^2)\ (\frac{a}{R})^2 \quad (4)$$

$$N_{II} = [2 + (8\cos^2\beta - 5)(\frac{a}{R})^2]\sin 2\beta \quad (5)$$

Due to the widespread application of rocks in everyday life and the destructive role of environmental factors in changing rock properties, there has always been a great interest in *in-situ* research or experimental simulation of natural processes. In the following, some studies on the effect of temperature and the number of heating–cooling cycles on the fracture toughness and physical and mechanical properties of rocks are reviewed.

Xiankai [12] studied the mode I, mode II and mixed-mode I-II fracture toughness of gypsum interlayers at different temperatures (20, 50, and 80°C) using CSTBD specimens in the case where the angle between the crack and loading directions was 0, 7, 15, 22, 30, 45, 60, 75, and 90°. The results showed a decrease in the fracture toughness of specimens as temperature increased. Feng *et al.* [1] determined the mode I, mode II, and mixed-mode I-II fracture toughness of semi-circular sandstone specimens through three-point bending tests. The tests were conducted at seven temperatures, namely the ambient temperature, 20, 100, 200, 300, 400, 500, and 600°C. The changes in the fracture toughness of the sandstone specimens were investigated at different temperatures. According to the results, the fracture toughness increased as the temperature increased from 20 to 100°C due to evaporation of surface water and microcrack closure. A further temperature increase over 100°C caused a decrease in the fracture toughness. For temperatures exceeding 500°C, the fracture toughness sharply decreased by about 46%. Hosseini [13] studied the effect of temperature and the number of heating–cooling cycles on the physical and mechanical properties of tuff, andesite and sandstone specimens. Two series of tests were conducted on the specimens. In the first series, the specimens experienced a heating–cooling cycle at ambient temperature (25°C), 100, 200, and 300°C. In the second series, the effect of the number of heating–cooling cycles on the velocity of longitudinal waves and tensile strength was investigated after 5, 10, and 15 heating–cooling cycles, in which the specimens were heated up to 100°C in the heating stage and then cooled down to the ambient temperature. The results of the first series of tests on four rock types showed that for a single heating–cooling cycle to the specimens, the velocity of longitudinal waves and tensile strength decreased by increasing temperature, whereas the porosity of specimens increased with increasing temperature. According to the results of the second series of tests, the velocity of longitudinal waves and tensile strength of specimens decreased with increasing the number of heating–cooling cycles. Funatsu *et al.* [11] investigated the effects of temperature and confining pressure on the mode II and mixed-mode I-II fracture toughness of sandstone specimens through three-point bending tests on semi-circular specimens at high temperatures (up to 200°C) and pressures (up to 5 MPa). According to the results, the fracture toughness decreased under atmospheric pressure from the room temperature to 75°C and then increased from 100 to 200°C. The fracture toughness of the sandstone specimens significantly increased with increasing the confining pressure. The fracture toughness of Kimachi sandstone increased by about 440% at 5 MPa relative to the atmospheric pressure. Lee *et al.* [14] determined the mixed-mode I-II/III fracture toughness of red and white granites from -50 to +240°C through three-point bending tests on semi-circular specimens. According to their results, increasing the temperature from -50 to +240°C had little effect on the modulus of elasticity of both granite rocks. In other words, no significant relationship was found between the temperature and modulus of elasticity in this temperature range. The mixed-mode I-II/III fracture toughness of both granite rocks decreased with increasing temperature. Al-Shayea and Khan [15] determined the mixed-mode I-II fracture toughness of straight notched Brazilian disc (SNBD) specimens at high pressures and temperatures. According to the results, K_{IC} was lower than K_{IIC} in all cases. The change in the mode I and mode II fracture toughness of the specimen with a diameter of 98 mm at different crack loading angles showed the significant influence of high confining pressures on the mode I and mode II fracture toughness and the insignificant impact of temperature up to 116°C.

The effects of temperature and number of heating–cooling cycles on the mode I, mode II and mixed-mode I-II fracture toughness of Lushan

sandstone were investigated through two series of tests. In the first series of tests for physical modeling fire, the rocks undergo a heating and cooling cycle, which means they are exposed to considerable heat first and then cooled after extinguishing the fire. In the fire, the temperature gradually rises, so these 7 temperatures are selected to consider the fracture toughness of sandstone at each temperature after extinguishing the fire. In the first series, the effect of temperature was studied in a heating–cooling cycle at the ambient temperature (25°C) and 60, 150, 200, 300, 500, and 700°C. In the second series of tests, the effect of number of heating–cooling cycles was investigated on the mode I, mode II and the mixed-mode I-II fracture toughness of Lushan sandstone at 150°C (for modeling hydraulic fracturing) and a crack inclination angle of 45°. A review of the literature indicates that most studies have focused on the effect of temperature and number of heating–cooling cycles on the mode I and mode II fracture toughness. The novelty of this study is to investigate the effect of temperature and number of heating–cooling cycles on the mixed-mode I-II fracture toughness, especially the fracture toughness of sandstone.

2- PREPARATION OF SPECIMENS

A thin section of rock specimen was studied under a polarizing microscope at 50x magnification to determine the types and percentage of minerals. Lushan sandstone samples were collected from Lalun Sandstone Formation, one of the largest formations in Iran. The rock is composed of 15% quartz, 15% calcite, 8% chert gravel, 7% feldspar, and 7% opaque minerals, and 48% of the cement matrix consists of fine quartz and clay (chlorite) grains. Cores with a diameter of 54 mm were prepared to determine the sandstone specimens' physical and mechanical properties. Cores with a diameter of 73 mm were prepared from the sandstone blocks to determine the fracture toughness.

A total of 200 discs was prepared by the cutterhead with an average thickness and diameter of 25 and 73 mm, respectively. A crack with an average length of 15 mm was created in the center of the Brazilian disc by water jet cutter (The cracks were created by Isatis Water jet company). The ratio of a/R = 0.2 was chosen because N_I and N_{II} (Equations 4 and 5) that denote the dimensionless intensity factors are valid for a/R≤.0.3.

A number of the discs were prepared to investigate the effect of temperature on the specimens previously subject to heating–cooling cycle. To this end, the discs were first placed in an oven and heated for 12 h. Three or four sandstone discs were placed in the oven (for modeling the heating process) to conduct the tests at each temperature and loading angle. The heating rate in the electrical furnace was 15 °C/min to simulate fire in accordance with a study by Mohtadi on fire in Sadaf Commercial Complex in Qeshm [16]. In the heating stage, the discs were heated at 25, 60, 150, 200, 300, 500, and 700°C, and then removed and cooled down to the ambient temperature. The second series of discs were prepared to investigate the effect of the number of heating–cooling cycles (1, 5, 10, 15, and 20 cycles) on the specimens heated at 150°C and cooled down to the ambient temperature for modeling hydraulic fracturing. The rate of temperature rise was 1-2°C/min in accordance with a study by Kim et al. [17]. In the first series, the tests were performed at each temperature at inclination angles of 0, 15, 28.8, 45, 60, 75 and 90°. In the second series, all tests were performed at a crack inclination angle of 45°.

3- RESULTS AND DISCUSSION

3-1- Physical and mechanical properties

The tests were performed under the ISRM standards [18] to determine the physical and mechanical properties of the sandstone. Several specimens were used in the tests to ensure the accuracy of the results. The mean results are presented in Table 1.

3-2- Effect of temperature on the sandstone properties

To find out the reasons for the changes in the fracture toughness, the tests were conducted based on the ISRM standards and included determining the effect of temperature on the effective porosity and the velocity of longitudinal waves [18]. Five tests were carried out on specimens for determining effective porosity and the longitudinal wave velocity at each temperature. Three tests were carried out on specimens for determining permeability.

Table 1. The mean physical and mechanical properties of the sandstone specimens

Poisson's ratio	Elastic modulus (GPa)	Cohesion (MPa)	Internal friction angle (°)	Longitudinal wave velocity (m/s)	Uniaxial compressive strength (MPa)	Dry specific weight (kN/m3)	Effective porosity (%)
0.26	23.98	15.43	55.59	4431	88	23.69	6.28

3-2-1- Effective porosity

Effective porosity includes interconnected voids capable of passing liquids. Porosity is created due to various reasons such as formation conditions (primary porosity) and secondary processes such as weathering and alteration (secondary porosity). The effective porosity is calculated as follows:

$$\Phi_e = \frac{V_e}{V_t} \quad (6)$$

where:
Φ_e: represents the effective porosity,
V_e: the volume of interconnected voids,
V_t: the total volume.

It was determined using the vacuum saturation and buoyancy technique [18]. The calculated effective porosities are presented in Table 2 and Figure 2.

As seen, the effective porosity decreases by 18% as temperatures rises from ambient temperature to 60°C due to closure of primary cracks. The closure of primary cracks continues up to 150°C, and thus the effective porosity significantly decreases by 43% relative to that at the ambient temperature. By subjecting the specimens to temperatures of 200, 300, and 500°C, new microcracks formed due to the stress concentration at the boundary of minerals resulting from their different thermal expansion coefficients. Additionally, formation of these microcracks is facilitated in the cooling stage due to the specimen's contraction, leading to an increase in the porosity. However, due to the presence of interstitial water and slow crack growth, the effective porosity steadily increases. Funatsu *et al.* conducted tests on sandstone discs and heated up the specimens to 200°C at a constant heating rate. The images from an optical microscope before and after heating indicate the formation of new cracks on the surface. This confirms the role of heating in this process [19]. Due to the increase in the number of microcracks, Lushan sandstone specimens' effective porosity at 700 °C increased to 2.36 times that at room temperature.

Table 2. The effective porosity at different temperatures

Temperature (°C)	Effective porosity (%)	$\frac{\emptyset_{et}}{\emptyset_{e25}}$ *
25	5.32	1
60	4.43	0.82
150	3.07	0.57
200	5.04	0.94
300	5.13	0.96
500	6.94	1.30
700	12.56	2.36

* $\emptyset_{et}$: effective porosity at 60, 150, 200, 300, 500, and 700°C
$\emptyset_{e25}$: effective porosity at 25°C

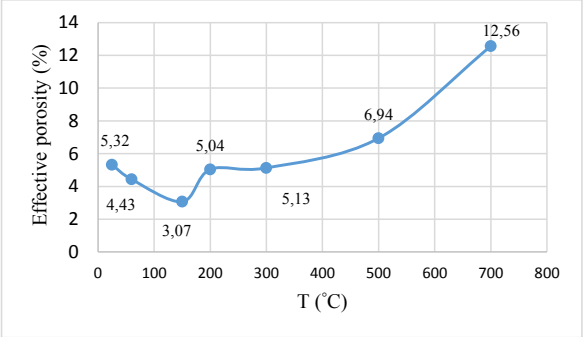

Figure 2. The effect of temperature on the effective porosity in a heating–cooling cycle

3-2-2- Effect of temperature on the velocity of longitudinal waves

The velocity of longitudinal waves was determined at different temperatures. The results for the sandstone specimens are presented in Table 3 and Figure 3.

As shown in Table 3 and Figure 3, as the temperature increases up to 60°C, the velocity of longitudinal waves increases by 0.4% relative to

Table 3. The velocity of longitudinal waves in the sandstone at different temperatures

Temperature (°C)	Longitudinal wave velocity (m/s)
25	4410.5
60	4427.9
150	4498.8
200	4396.6
300	3774.2
500	2847.3
700	1499.6

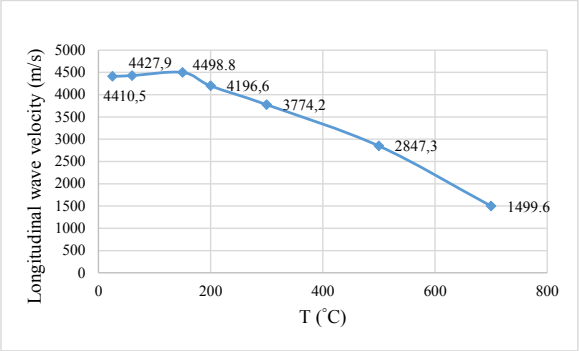

Figure 3. The effect of temperature on the velocity of longitudinal waves in a heating–cooling cycle

the ambient temperature due to a decrease in the effective porosity. By subjecting the sandstone specimen to a temperature of 150°C, the velocity of longitudinal waves increased by 2% relative to the ambient temperature due to closure of microcracks, evaporation of surface water, and reduction of effective porosity. The velocity of longitudinal waves at 200, 300, and 500°C decreased, respectively, by 5, 16, and 36% due to formation of microcracks and the increased the effective porosity. At 700°C, the velocity of longitudinal waves significantly decreased by 66% relative to the ambient temperature due to the increased density of microcracks and the significant increase in the effective porosity.

3-2-3- Effect of temperature on the permeability of sandstone

In addition to determining the effective porosity and longitudinal waves velocity, the specimens' permeability was also determined to prove the formation of the closure of microcracks.

Equation 7 has been used to calculate the permeability [20]. This relationship is valid for determining permeability when the fluid flow is steady state.

$$k = \frac{\mu q L}{\Delta p A} \quad (7)$$

Where:
μ: Dynamic viscosity of fluid (water) (MPa.s),
q: flow rate in terms (m^3/s),
L: Specimen length (m),
A: Sample cross section (m^2),
Δp: the difference in fluid pressure between inlet and outlet (MPa).

The constant head test is used to measure permeability. The fluid used is water, and the longitudinal permeability of the samples is determined.

At each temperature, 3 experiments were performed and the average results are listed in the Table 4.

Table 4. The permeability in the sandstone at different temperatures

Temperature (°C)	Permeability (m^2)
25	7.65×10^{-16}
60	7.05×10^{-16}
150	6.85×10^{-16}
200	7.97×10^{-16}
300	15.65×10^{-16}
500	95.15×10^{-16}
700	300.17×10^{-16}

Up to 150 °C, the sandstone's permeability was reduced and then was increased with the temperature increasing at the heating-cooling process. Permeability changes in the heating-cooling process were consistent with the variations of the velocity of longitudinal waves.

3-3- Effect of temperature on the mode I, mode II and the effective mixed-mode I-II fracture toughness

A total of 200 sandstone disc specimens was

tested to determine the effect of temperature on fracture toughness. To this end, the specimens were tested at 60, 25, 150, 200, 300, 500, and 700°C as well as seven different crack inclination angles (0, 15, 28.8, 45, 60, 75, and 90°). Because N_I value [8] is zero at the crack inclination angle of 28.8, and as a result, the fracture mode is a pure shear mode. To ensure the accuracy of the results, three or four specimens were used in each case. The Figure 4 schematically shows the geometry and loading conditions on the specimen. First the specimen was placed in the axial loading jack. Then the loading continued until the specimen was fractured, and the data recording device recorded the fracture load. The fracture toughness was calculated from Equations 1, 2 and 3, and the results are presented in Tables 5, 6, 7 and 8 and Figures 5, 6, and 7.

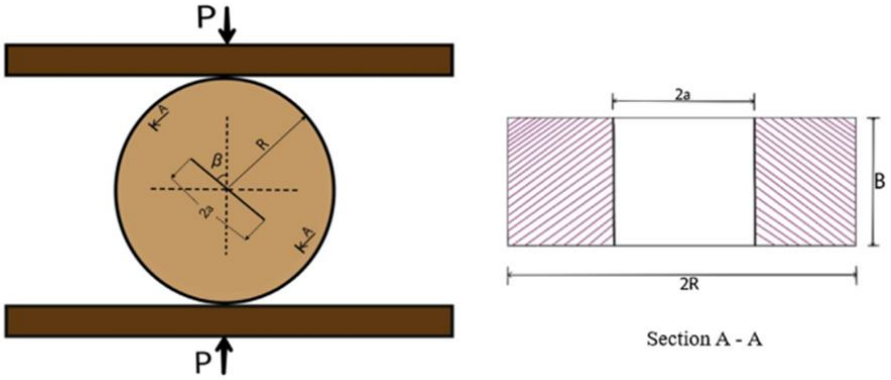

Figure 4. A centrally cracked Brazilian disc specimen under compression

Table 5. Effect of temperature on the mode I, mode II and the effective mixed-mode I-II fracture toughness

Crack Inclination angle (°)	Temperature (°C)	K_{IC} average (Mpa.√m)	K_{IIC} averge (Mpa.√m)	$K_{(I-II)C}$ averge (Mpa.√m)	K_{IC} Standard deviation (Mpa.√m)	K_{IIC} Standard deviation (Mpa.√m)	$K_{(I-II)C}$ Standard deviation (Mpa.√m)
pure mode I (α=0)	25	0.82	0.00	0.82	0.010	0.000	0.010
	60	0.88	0.00	0.88	0.061	0.000	0.061
	150	1.03	0.00	1.03	0.028	0.000	0.028
	200	0.88	0.00	0.88	0.083	0.000	0.083
	300	0.86	0.00	0.86	0.019	0.000	0.019
	500	0.74	0.00	0.74	0.023	0.000	0.023
	700	0.31	0.00	0.31	0.041	0.000	0.041
Mixed mode Loading (α=15)	25	0.51	0.78	0.93	0.041	0.064	0.076
	60	0.57	0.86	1.04	0.008	0.012	0.015
	150	0.65	1.00	1.20	0.006	0.009	0.011
	200	0.60	0.93	1.11	0.022	0.034	0.040
	300	0.57	0.89	1.06	0.038	0.054	0.066
	500	0.47	0.73	0.87	0.015	0.018	0.023
	700	0.19	0.29	0.35	0.021	0.032	0.038

Table 5 (Continued). Effect of temperature on the mode I, mode II and the effective mixed-mode I-II fracture toughness

Crack Inclination angle (°)	Temperature (°C)	K_{IC} average (Mpa.√m)	K_{IIC} averge (Mpa.√m)	$K_{(I-II)C}$ averge (Mpa.√m)	K_{IC} Standard deviation (Mpa.√m)	K_{IIC} Standard deviation (Mpa.√m)	$K_{(I-II)C}$ Standard deviation (Mpa.√m)
pure mode II (α=28.8)	25	0.02	1.26	1.26	0.005	0.016	0.017
	60	0.01	1.31	1.31	0.008	0.110	0.110
	150	0.01	1.42	1.42	0.003	0.060	0.060
	200	0.01	1.34	1.34	0.010	0.131	0.132
	300	0.01	1.27	1.27	0.009	0.086	0.086
	500	0.00	1.08	1.08	0.002	0.046	0.046
	700	0.00	0.45	0.45	0.002	0.038	0.038
Mixed mode Loading (α=45)	25	-0.85	1.50	1.72	0.066	0.102	0.122
	60	-0.88	1.53	1.76	0.071	0.108	0.129
	150	-1.00	1.73	1.99	0.061	0.094	0.112
	200	-0.88	1.52	1.76	0.055	0.098	0.112
	300	-0.72	1.25	1.44	0.085	0.142	0.166
	500	-0.66	1.15	1.32	0.018	0.036	0.040
	700	-0.27	0.49	0.56	0.004	0.011	0.011
Mixed mode Loading (α=60)	25	-1.40	1.11	1.79	0.073	0.055	0.091
	60	-1.50	1.19	1.92	0.086	0.063	0.106
	150	-1.65	1.30	2.10	0.052	0.030	0.060
	200	-1.40	1.11	1.79	0.074	0.053	0.090
	300	-1.34	1.07	1.72	0.094	0.077	0.121
	500	-1.04	0.82	1.32	0.104	0.083	0.133
	700	-0.45	0.36	0.58	0.042	0.035	0.055
Mixed mode Loading (α=75)	25	-1.77	0.60	1.87	0.130	0.046	0.138
	60	-1.84	0.63	1.94	0.082	0.024	0.085
	150	-1.99	0.68	2.10	0.103	0.027	0.107
	200	-1.92	0.65	2.02	0.134	0.043	0.141
	300	-1.84	0.63	1.94	0.062	0.021	0.066
	500	-1.71	0.58	1.81	0.156	0.050	0.164
	700	-0.77	0.26	0.81	0.034	0.012	0.036
Mixed mode Loading (α=90)	25	-1.89	0.00	1.89	0.103	0.000	0.103
	60	-2.00	0.00	2.00	0.031	0.000	0.031
	150	-2.23	0.00	2.23	0.257	0.000	0.257
	200	-2.06	0.00	2.06	0.006	0.000	0.006
	300	-1.95	0.00	1.95	0.089	0.000	0.089
	500	-1.88	0.00	1.88	0.135	0.000	0.135
	700	-0.90	0.00	0.90	0.073	0.000	0.073

According to Tables 5, 6, 7 and 8 and Figures 5, 6 and 7, the mode I, mode II and effective value of the mixed-mode I-II fracture toughness increase at all angles from the ambient temperature up to 150°C. Up to 150°C, the effective porosity and the permeability decreased due to the closure of pre-existing cracks. As a result of the closure of the pre-existing cracks, the fracture toughness increased.

Table 6. The ratio of changes in the mode I fracture toughness

Crack inclination angle (°)	$\frac{K_{IC60}}{K_{IC25}}$	$\frac{K_{IC150}}{K_{IC25}}$	$\frac{K_{IC200}}{K_{IC25}}$	$\frac{K_{IC300}}{K_{IC25}}$	$\frac{K_{IC500}}{K_{IC25}}$	$\frac{K_{IC700}}{K_{IC25}}$
0	1.07	1.26	1.07	1..05	0.91	0.39
15	1.13	1.28	1.18	1.13	0.92	0.37
28.8	0	0	0	0	0	0
45	1.03	1.17	1.04	0.85	0.77	0.32
60	1.07	1.17	1.00	0.96	0.74	0.32
75	1.04	1.12	1.08	1.04	0.97	0.44
90	1.06	1.18	1.09	1.04	0.99	0.48

Table 7. The ratio of changes in the mode II fracture toughness

Crack inclination angle (°)	$\frac{K_{IIC60}}{K_{IIC25}}$	$\frac{K_{IIC150}}{K_{IIC25}}$	$\frac{K_{IIC200}}{K_{IIC25}}$	$\frac{K_{IIC300}}{K_{IIC25}}$	$\frac{K_{IIC500}}{K_{IIC25}}$	$\frac{K_{IIC700}}{K_{IIC25}}$
0	0	0	0	0	0	0
15	1.10	1.28	1.19	1.14	0.93	0.37
28.8	1.04	1.13	1.06	1.01	0.86	0.36
45	1.02	1.15	1.02	0.84	0.76	0.32
60	1.07	1.17	1.00	0.97	0.74	0.32
75	1.04	1.13	1.08	1.05	0.96	0.43
90	0	0	0	0	0	0

Table 8. The ratio of changes in effective value of the mixed-mode I-II fracture toughness

Crack inclination angle (°)	$\frac{K_{eff60}}{K_{eff25}}$	$\frac{K_{eff150}}{K_{eff25}}$	$\frac{K_{eff200}}{K_{eff25}}$	$\frac{K_{eff300}}{K_{eff25}}$	$\frac{K_{eff500}}{K_{eff25}}$	$\frac{K_{eff700}}{K_{eff25}}$
0	1.07	1.26	1.07	1.05	0.91	0.39
15	1.11	1.28	1.19	1.13	0.93	0.37
28.8	1.04	1.13	1.06	1.01	0.86	0.36
45	1.02	1.16	1.02	0.84	0.77	0.32
60	1.07	1.17	1.00	0.96	0.74	0.32
75	1.04	1.13	1.08	1.04	0.97	0.44
90	1.06	1.18	1.09	1.04	0.99	0.48

This is consistent with the results of Funatsu *et al.* [19] on clay rock, who reported an increase in the fracture toughness up to 125°C. According to Al-Shayea [21], the facture toughness of limestone increased by about 25% at 116°C relative to the ambient temperature. The fratcure toughness of the sandstones decreased from 200 to 500°C due to formation of microcracks. Microcracks' formation is due to increased expansion of the constituent particles and different coefficient of thermal expansion. This difference causes non-uniform deformation of the particles and the formation of new micro-cracks in the rock specimens. The effective porosity and the permeability were

determined to prove the formation of new microcracks in the rock specimens. The increase of the effective porosity and permeability and decrease of the velocity of longitudinal waves from 200 to 500°C is due to the formation of new microcracks. As a result of the formation of new micro-crack, the fracture toughness decreased.

As mentioned in Section 2, 15% of the sandstone mineral composition is calcite. At 700°C, evaporation of interstitial water, conversion of $CaCO_3$ (calcite) to CaO, and CO_2 emissions [22] lead to a change in the color, the formation of microcracks, and rapid reduction of the fracture toughness.

Conversion of $CaCO_3$ (calcite) to CaO, and CO_2 emissions cause a sharp increase in the density of microcracks.

Figure 7 shows an increase in effective value of the mixed-mode I-II fracture toughness with increasing the crack inclination angle. Figure 8 displays the images of the specimens after loading at different crack inclination angles. As temperature rises, the sandstone color changes from gray to brown due to clays' calcination in the sandstone. The crack propagation began from the pre-existing crack tip at inclination angles less than 45°. At inclination angles equal to or larger than 45°, the wing cracks propagate away from the crack tip. When the loading angle reaches 90°, the crack propagation angle reaches its maximum value of 90°.

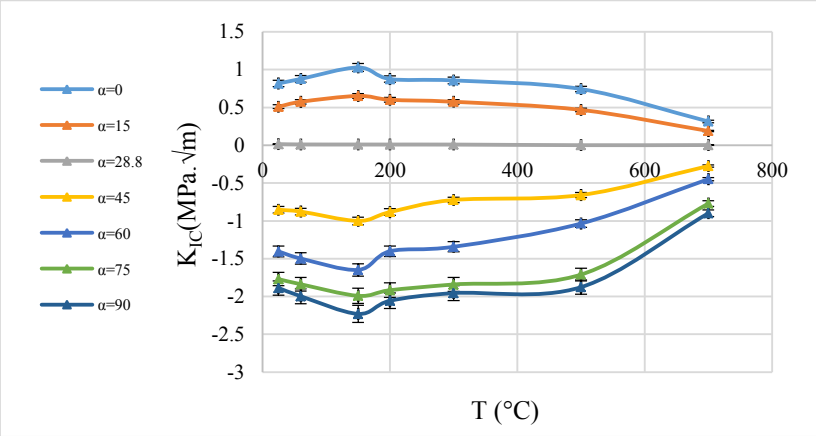

Figure 5. The effect of temperature on the mode I fracture toughness

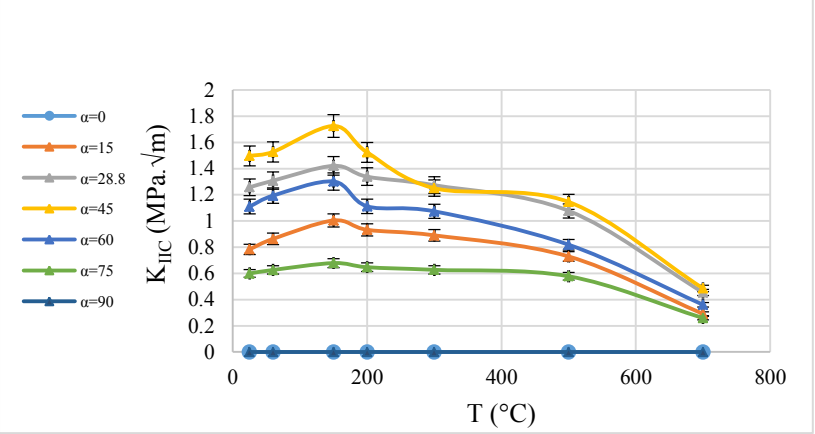

Figure 6. The effect of temperature on the mode II fracture toughness

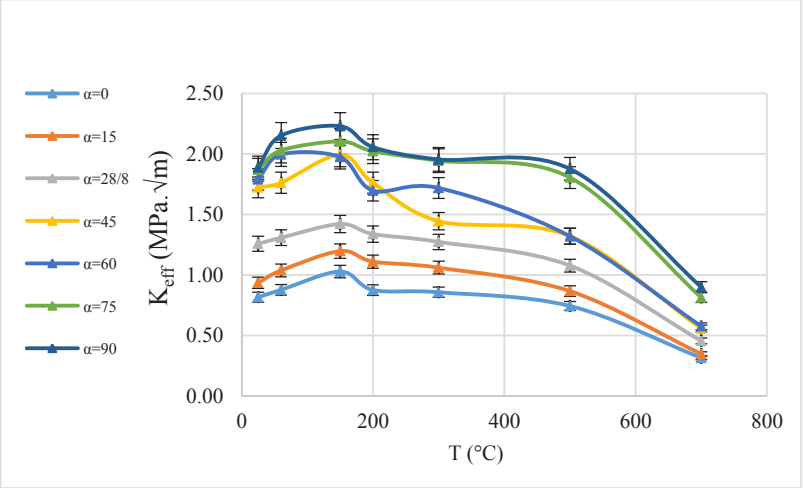

Figure 7. The effect of temperature on the effective mixed-mode I-II fracture toughness

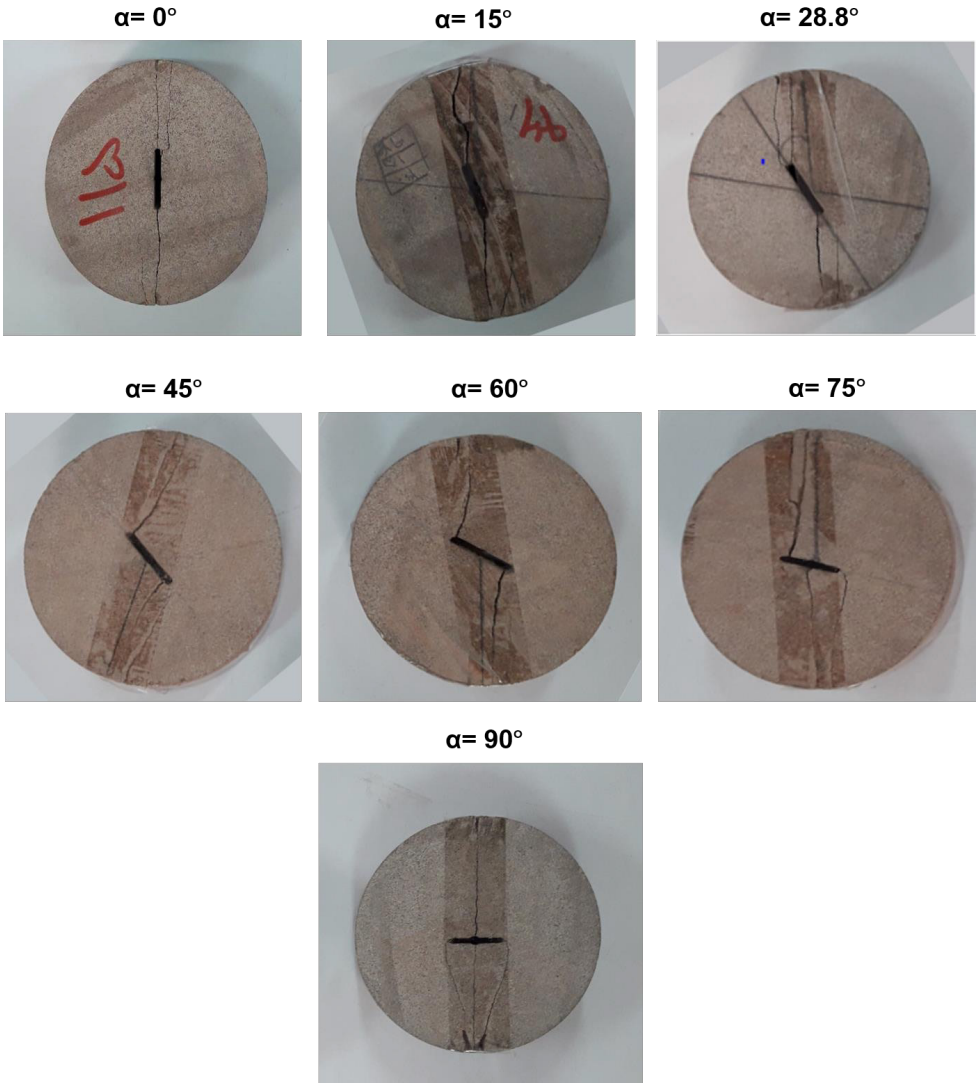

Figure 8. Crack propagation in the sandstone specimens after loading

3-4- Effect of number of heating–cooling cycles on the sandstone properties

In this section, the results of tests conducted to investigate the effect of the number of heating–cooling cycles on the mixed-mode I-II fracture toughness of the sandstone specimens are discussed. The specimens were heated in an oven at 150°C and then cooled down to the ambient temperature after 1, 5, 10, 15, and 20 cycles. The effective porosity and the velocity of longitudinal waves were determined according to the ISRM standards [18]. To investigate the reason of changes in the fracture toughness due to number of heating–cooling cycles, the effective porosity and velocity of longitudinal waves were determined.

3-4-1- Effect of number of heating–cooling cycles on the effective porosity

The effective porosity and the velocity of longitudinal waves were determined to prove closure of the pre-existing cracks or formation of new microcracks after 1, 5, 10, 15, and 20 cycles. The effective porosity is presented in Figure 9.

As temperature rises to 150°C in a heating–cooling cycle, the effective porosity decreases by 3% due to the closure of joints and cracks. However, thermal shocks cause microcracks' formation in the specimens after 5, 10, 15, and 20 cycles. After each heating–cooling cycle, the effective porosity increased by 4, 7, 21, 23% in the 5th, 10th, 15th, and 20th cycles relative to the cycle 0.

3-4-2- Effect of number of heating–cooling cycles on the velocity of longitudinal wave

The velocity of longitudinal waves in the sandstone specimens was also determined. Figure 10 shows the effect of the number of heating–cooling cycles on the velocity of longitudinal waves.

The velocity of longitudinal waves increased in the first cycle due to the closure of microcracks and reduction of effective porosity. In the 5th cycle, the velocity of longitudinal waves decreased due to the formation of microcracks caused by thermal shocks in each heating–cooling cycle. The velocity of longitudinal waves decreased in the 10th, 15th and 20th cycles due to microcracks' formation. It can, therefore, be concluded that except for the first cycle, the velocity of longitudinal waves decreases in other cycles due to microcracks' formation.

3-5- Effect of number of heating–cooling cycles on the mode I, mode II and the effective value of the mixed-mode I-II fracture toughness

Equations 1, 2 and 3 were used to calculate the fracture toughness of the SNBD sandstone specimens. An angle of 45° was considered between the loading and crack propagation directions. The diameter and thickness of specimens were 74 and 24 mm, respectively. Three specimens were used in each cycle to ensure the accuracy of the results. Table 8 and Figure 11 show the mixed-mode I-II

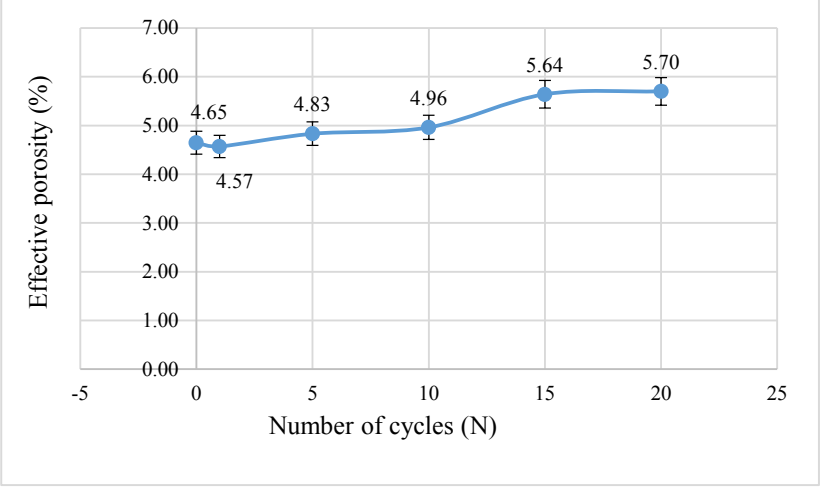

Figure 9. Effect of number of heating–cooling cycles on the effective porosity

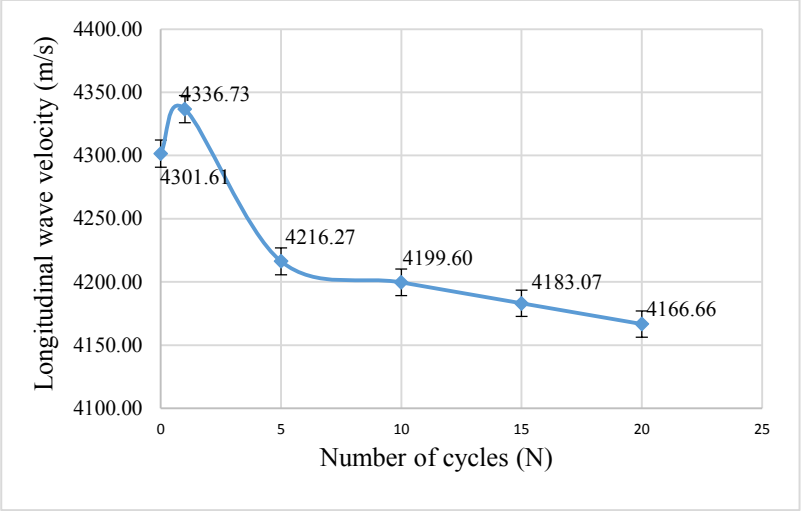

Figure 10. The effect of number of heating–cooling cycles on the velocity of longitudinal waves in the sandstone specimens

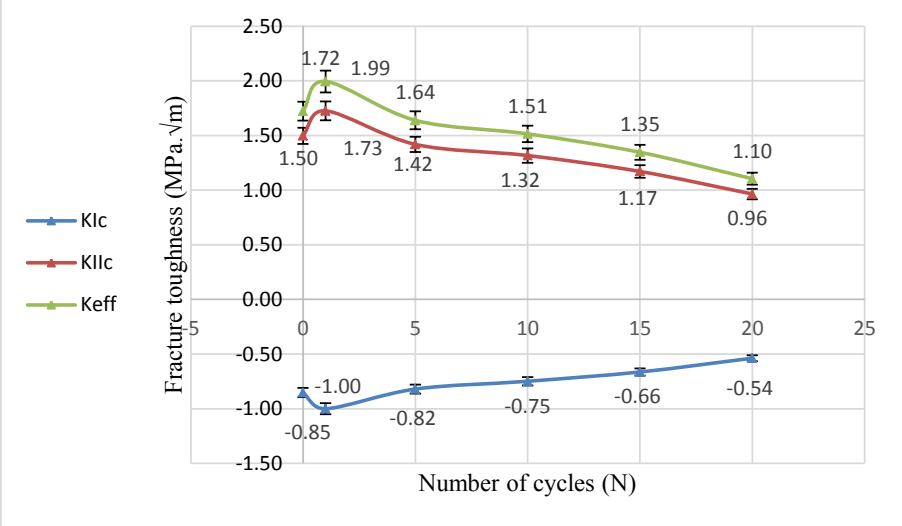

Figure 11. The fracture toughness of the sandstone specimens as a function of the number of heating–cooling cycles at a crack inclination angle of 45°

fracture toughness of the sandstone specimens in different cycles.

As clearly seen in Figure 11 and Table 8, the mode I, mode II, and the effective mixed-mode I-II fracture toughness of specimens in the first cycle increase, respectively, by 17, 15, and 16% relative to the 0th cycle due to the closure of microcracks and evaporation of pore water. However, the density of microcracks increases from the 5th cycle onwards due to thermal shocks. As a result, the mode I fracture toughness of the specimens after 5, 10, 15, and 20 heating–cooling cycles decreased, respectively, by 3.9, 12.2, 22.2, and 36.9% compared to that in the 0th cycle (ambient temperature). The mode II fracture toughness of the specimens decreased by 5.2, 12.1, 21.8, and 35.6% compared to that in the 0th cycle (ambient temperature). The effective mixed-mode I-II fracture toughness of the specimens decreases by 4.9, 12.1, 21.9, and 35.9% compared to that in the 0th cycle (ambient temperature), which well corresponds to the changes in the

effective porosity and velocity of longitudinal waves. Finally, it can be concluded that as the temperature rises to 150°C in the heating–cooling cycle, the effective porosity decreases, and the velocity of longitudinal waves increases due to the closure of cracks. As a result of the closure of the pre-existing cracks, the fracture toughness increases.

After 5, 10, 15, and 20 cycles, the effective porosity increased and the velocity of longitudinal waves decreased due to formation of new microcracks. As a result of the formation of new microcracks, the fracture toughness decreased.

3-6- Effect of crack inclination angle on the fracture toughness

The fracture toughness varies by changing the loading angle relative to the crack direction (crack inclination angle). Figures 12, 13, and 14 show the changes in the fracture toughness of the sandstone specimens at crack inclination angles of 0, 15, 28.8, 45, 60, 75, and 90°.

As seen in Figure 12, the mode I fracture toughness decreases at 25, 60, 150, 200, 500, and 700°C with a negative slope. The fracture toughness approaches 0 at all temperatures at a crack inclination angle of 28.8°. The fracture

Table 8. The changes in the fracture toughness of the sandstone specimens with the number of heating–cooling cycles relative to the 0th cycle at a crack inclination angle of 45°

Cycle	Mode I fracture toughness	Mode II fracture toughness	Effective value of the mixed-mode I-II fracture toughness
Ratio of 1st cycle to 0th cycle	+ 17 %	+15 %	+16 %
Ratio of 5th cycle to 0th cycle	-3.9 %	-5.2 %	-4.9 %
Ratio of 10th cycle to 0th cycle	-12.2 %	-12.1 %	-12.1 %
Ratio of 15th cycle to 0th cycle	-22.2 %	-21.8 %	-21.9 %
Ratio of 20th cycle to 0th cycle	-36.9 %	-35.6 %	-35.9 %

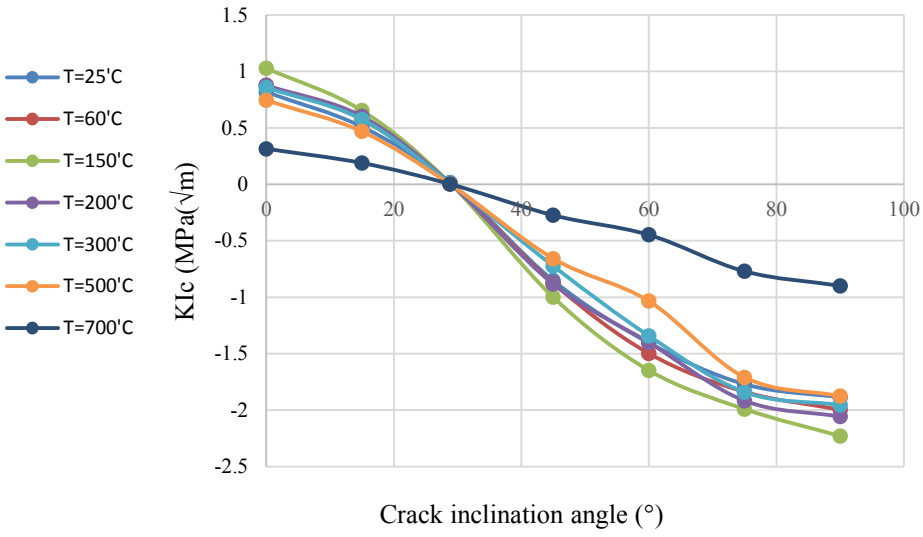

Figure 12. The effect of crack inclination angle on the mode I fracture toughness

toughness increases from 45 to 90° with a negative angle, and the maximum fracture toughness is observed at a crack inclination angle of 90° relative to the crack direction. The mode of fracture changes from opening mode (mode I) at the crack inclination angle of zero degree to mixed mode (tension-shear) at the crack inclination angle of less than 28.8°. The mode of fracture changes from tension-shear to compression-shear (The minus sign behind the fracture toughness values indicates the mode of fracture is compression-shear.) at the crack inclination angle of greater than 28.8°. A minimum mode II fracture toughness of 0 is observed at an inclination angle of 0°. As the crack inclination angle increases, the fracture toughness increases. The maximum fracture toughness is observed at an inclination angle of 45°. With further increase in the inclination angle, the fracture toughness decreases and approaches 0 at a crack inclination angle of 90° (Figure 13). As shown in Figure 14, the effective mixed-mode I-II fracture toughness increases at all temperatures

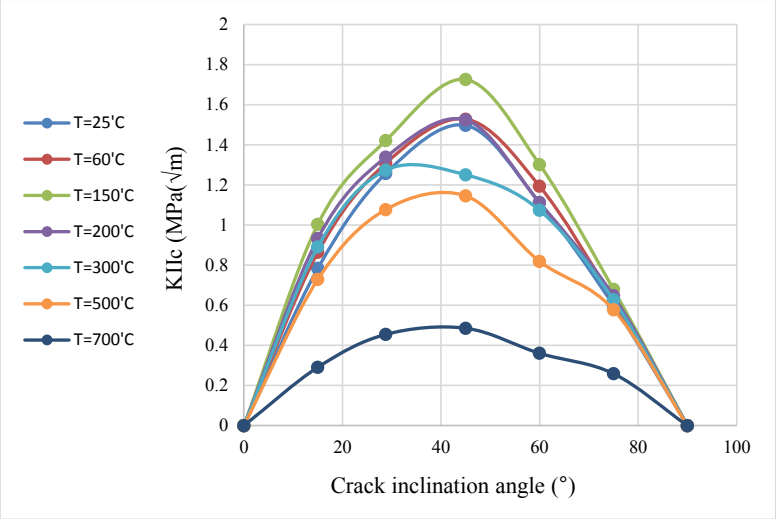

Figure 13. The effect of crack inclination angle on the mode II fracture toughness

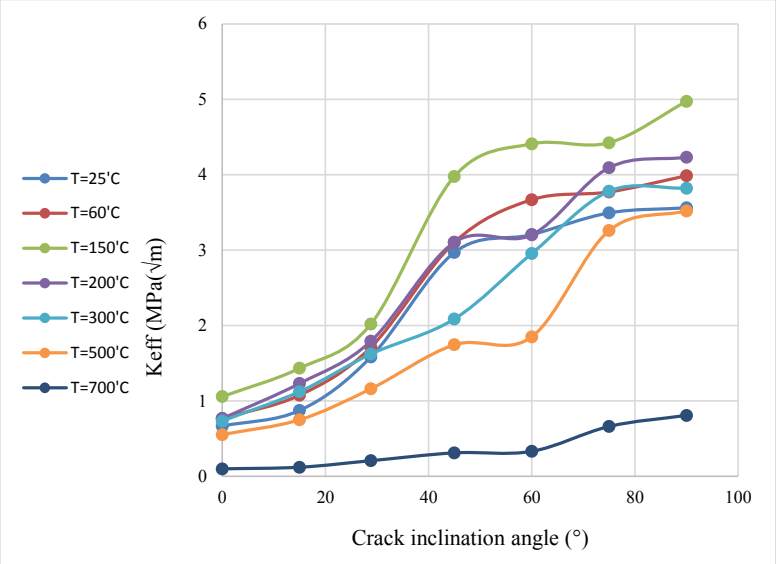

Figure 14. The effect of crack inclination angle on the effective value of the mixed-mode I-II fracture toughness

with increasing the crack inclination angle. The lowest and highest fracture toughness are observed, respectively, at inclination angles of 0 and 90°.

4- CONCLUSION

Two series of tests were conducted in this study. In the first series, the effect of temperature in a heating–cooling cycle was investigated at the ambient temperature (25), 60, 150, 200, 300, 500, and 700°C and crack inclination angles of 0, 15, 28.8, 45, 60, 75, and 90°. At all inclination angles:

- The highest and lowest mode I, mode II, and mixed-mode I-II fracture toughness were observed at 150 and 700°C, respectively.
- The mode I, mode II and the effective mixed-mode I-II fracture toughness increased at 60 and 150°C due to the closure of microcracks and reduction of effective porosity. The highest increase in the fracture toughness was observed at 150°C.
- Due to the presence of interstitial water at 200 and 300°C, the fracture toughness did not change significantly. As a result, the mode I, mode II and the effective mixed-mode I-II fracture toughness of the sandstone specimens decreased with a slight slope due to microcracks' formation.
- Due to evaporation of interstitial water, conversion of $CaCO_3$ to CaO and CO_2 emissions, and formation of a large number of microcracks in the specimens, the mode I, mode II and the effective mixed-mode I-II fracture toughness of the sandstone specimens significantly decreased at 700°C.
- At all temperatures and by increasing the crack inclination angle, the mode I fracture toughness decreased with a negative slope, approached 0 at 28.8°, and eventually increased with a negative slope as the angle increased from 45 to 90°.
- The mode II fracture toughness was at its lowest at an inclination angle of 0°, but increased with increasing the crack inclination angle, reaching its highest at an inclination angle of 45°. Further increases in the inclination angle decreased the mode II fracture toughness, reaching 0 at an inclination angle of 90°.
- The effective mixed-mode I-II fracture toughness increased at all temperatures with increasing the crack inclination angle. The lowest and highest mixed-mode I-II fracture toughness were, respectively, observed at inclination angles of 0 and 90°.

In the second series of experiments, the effect of the number of heating–cooling cycle was investigated on the mode I, mode II and mixed-mode I-II fracture toughness of the sandstone specimens at 150°C and an inclination angle of 45°. According to the results:

- The effective mixed-mode I-II fracture toughness of the sandstone specimens in the first cycle increased by 16% relative to the 0^{th} cycle. As the number of heating–cooling cycles increased from 5, 10, 15, and 20, the effective mixed-mode I-II fracture toughness of the sandstone specimens decreased, respectively, by 4.9, 12.1, 21.9, and 35.9% relative to the 0^{th} cycle.
- The loading angle effect relative to the crack direction on the fracture toughness was investigated at inclination angles of 0, 15, 28.8, 45, 60, 75, and 90°. With increasing the crack inclination angle, the mode II fracture toughness increased up to 45° and then decreased. Furthermore, the mode of fracture changes from opening mode (mode I) at the crack inclination angle of zero degree to mixed mode (tension-shear) at the crack inclination angle of less than 28.8°. The mode of fracture changes from tensile-shear to compression-shear at the crack inclination angle of greater than 28.8°.

5- REFERENCES

[1] Feng, G., Kang, Y., Chen, F., Liu, Y. W., and Wang, X. C. (2018). *"The influence of temperatures on mixed-mode (I+ II) and mode-II fracture toughness of sandstone"*. Engineering Fracture Mechanics, 189: 51-63.

[2] Lim, I. L., Johnston, I. W., and Choi, S. K. (1994). *"Assessment of mixed-mode fracture toughness testing methods for rock"*. In International Journal of Rock Mechanics and Mining Sciences & Geomechanics Abstracts, Pergamon, 31(3): 265-272.

[3] Haeri, H., and Marji, M. F. (2016). *"Simulating the crack propagation and cracks coalescence underneath*

TBM disc cutters". Arabian Journal of Geosciences, 9(2): 124.

[4] Kundu, T. (2008). *"Fundamentals of fracture mechanics"*. CRC press, pp. 283.

[5] Marji, M. F. (2014). *"Numerical analysis of quasi-static crack branching in brittle solids by a modified displacement discontinuity method"*. International Journal of Solids and Structures, 51(9): 1716-1736.

[6] Awaji, H., and Sato, S. (1978). *"Combined Mode Fracture Toughness Measurement by the Disc Test, J. of Engng"*. Journal of Engineering Materials and Technology, 100: 175-182.

[7] Khan, K. (1998). *"Fracture toughness investigation of an indigenous limestone rock formation"*. Doctoral Dissertation, King Fahd University of Petroleum and Minerals, pp. 209.

[8] Atkinson, C., Smelser, R. E., and Sanchez, J. (1982). *"Combined mode fracture via the cracked Brazilian disk test"*. International Journal of Fracture, 18(4): 279-291.

[9] Chong, K., and Kuruppu, M. (1984). *"New specimen for fracture toughness determination for rock and other materials"*. International Journal of Fracture, 26: R59–R62.

[10] Aliha, M. R. M., Mahdavi, E., and Ayatollahi, M. R. (2017). *"The influence of specimen type on tensile fracture toughness of rock materials"*. Pure and Applied Geophysics, 174(3): 1237-1253.

[11] Funatsu, T., Kuruppu, M., and Matsui, K. (2014). *"Effects of temperature and confining pressure on mixed-mode (I–II) and mode II fracture toughness of Kimachi sandstone"*. International Journal of Rock Mechanics and Mining Sciences, 67: 1-8.

[12] Xiankai, B., Meng, T., and Jinchang, Z. (2018). *"Study of mixed mode fracture toughness and fracture trajectories in gypsum interlayers in corrosive environment"*. Royal Society Open Science, 5(1): 171374.

[13] Hosseini, M. (2017). *"Effect of temperature as well as heating and cooling cycles on rock properties"*. Journal of Mining and Environment, 8(4): 631-644.

[14] Li-yun, L., Zhi-qiang, X., Ming-xiu, L., Yi, L., Chen, F., and Tie-Wu, T. (2013). *"An experimental study of I-II-III mixed mode crack fracture of rock under different temperature"*. In 13th International Conference on Fracture June, 16-21.

[15] Al-Shayea, N. A., and Khan, K. (2001). *"Fracture toughness envelope of a limestone rock at high confining pressure and temperature"*. In 10th International Conference on Fracture, Hawaii, 2-6.

[16] Mohtadi, V. R., and Mohtadi, A. R. (2015). *"The results of ultrasonic testing on the concrete structure damaged in a fire accident, Sadaf Commercial Complex, Qeshm"*. Civil Journal, Retrofitting and Improvement, 31: 79-83.

[17] Kim, K., Kemeny, J., and Nickerson, M. (2014). "Effect of rapid thermal cooling on mechanical rock properties". Rock Mechanics and Rock Engineering, 47: 2005-2019.

[18] Ulusay, R. (Ed.). (2014). *"The ISRM suggested methods for rock characterization, testing and monitoring: 2007-2014"*. Springer, pp. 265.

[19] Funatsu, T., Seto, M., Shimada, H., Matsui, K., and Kuruppu, M. (2004). *"Combined effects of increasing temperature and confining pressure on the fracture toughness of clay bearing rocks"*. International Journal of Rock Mechanics and Mining Sciences, 41(6): 927-938.

[20] Boulin, P. F., Bretonnier, P., Gland, N., and Lombard, J. M. (2012). *"Contribution of the steady state method to water permeability measurement in very low permeability porous media"*. Oil & Gas Science and Technology–Revue d'IFP Energies nouvelles, 67(3): 387-401.

[21] Al-Shayea, N. (2002). *"Comparing reservoir and outcrop specimens for mixed mode I–II fracture toughness of a limestone rock formation at various conditions"*. Rock Mechanics and Rock Engineering, 35(4): 271-297.

[22] Lü, C., Sun, Q., Zhang, W., Geng, J., Qi, Y., and Lu, L. (2017). *"The effect of high temperature on tensile strength of sandstone"*. Applied Thermal Engineering, 111: 573-579.